JOURNAL OF PHYSICAL ORGANIC CHEMISTRY, VOL. 10, 113–120 (1997)

AB INITIO CALCULATIONS OF THE POTENTIAL ENERGY SURFACES FOR THE UNIMOLECULAR DISSOCIATION REACTION OF ETHYLENE OXIDE

JOSEPH J. BELBRUNO

Department of Chemistry, Dartmouth College, Hanover, New Hampshire 03755, USA

***Ab initio* calculations, including electron correlation, were employed to compute the geometries and energies of all stable C_2H_4O species, as well as four transition states along the potential surfaces connecting oxirane to the unimolecular dissociation products. The calculations indicate that the primary step in the major reaction observed experimentally is the isomerization of oxirane along the ground-state potential surface to acetaldehyde. Calculations indicate that the experimental reaction products are derived from unimolecular decomposition on the acetaldehyde S_0 surface ($CH_4 + CO$) or, after intersystem crossing, along the lowest triplet state of acetaldehyde ($CH_3 + HCO$). Additional pathways connecting oxirane to a number of less energetically favorable ring-opened or fragmentation products are also presented. © 1997 by John Wiley & Sons, Ltd.**

J. Phys. Org. Chem. **10**, 113–120 (1997) No. of Figures: 3 No. of Tables: 4 No. of References: 22

Keywords: ethylene oxide; potential energy surfaces; *ab initio* calculations

Received 1 February 1996; revised September 1996; accepted 18 September 1996

INTRODUCTION

The thermal reactivity of oxirane has been examined under a number of different experimental conditions and several different primary reaction mechanisms have been proposed. Among the earliest studies, Mueller and Walters[1] reported on the thermal reaction of several hundred torr of oxirane at temperatures up to 700 K. They speculated that hydrogen abstraction by methyl radicals was responsible for a large fraction of the decomposition of the starting material. Crocco *et al*.[2] employed temperatures as high as 1200 K and suggested that the critical reaction, initiating chain decomposition of oxirane, was the formation of formaldehyde and methylene radicals from a ring-opened oxirane. Neufeld and Blades[3] used approximately 1 atm of oxirane and temperatures up to 750 K. They reported that the observations were consistent with the initial formation of an excited acetaldehyde molecule, via thermally induced isomerization, followed by either stabilization of the primary product or subsequent decomposition to methyl and formyl radicals. Benson[4] also reported kinetic data consistent with the initial formation of a hot acetaldehyde intermediate and proposed a complex reaction scheme to account for all of the remaining products. Lifshitz and Ben-Hamou[5] used a shock tube to study high-pressure reactions of ethylene oxide at temperatures up to 1200 K. These studies produced, in addition to acetaldehyde and alkenes, methane and carbon monoxide. They proposed that the last two products result from the direct rearrangement/dissociation of the intermediate acetaldehyde.

There have been computational studies of the various electronic states of oxirane[6–10] and acetaldehyde,[11–15] but these reports did not consider the entire system of C_2H_4O isomers, nor did they optimize the geometries of all the relevant intermediates and transition states. In addition, only two of these reports used models with electron correlation. In both instances, the MP2 methods were employed and this theoretical model may not be appropriate for a system in which diradical intermediates are formed. The likelihood of low-lying states mixing with the radical ground states is significant. Therefore, a model that correctly mixes in these additional configurations, such as MC-SCF or CI methods, is generally required.[16] The current *ab initio* calculations are the first to involve complete optimization at a level as high as QCISD/6–31G* for not only the stable geometries, but also the transition structures connecting many of those stable species. The calculations confirm that the initial step in the reaction of oxirane is isomerization to the acetaldehyde structural isomer.

COMPUTATIONAL METHODS

All *ab initio* calculations were carried out using the Gaussian 92 suite of programs.[17] Initial optimizations were

Contract grant sponsor: Pittsburgh Superconducting Center; Contract grant number: CHE950013P

CCC 0894–3230/97/020113–08 $17.50

performed at the HF/6–31G* level, followed by MP2/6–31G* optimization. MP2/6–31G* harmonic vibrational frequencies were computed, using analytic second derivatives, to confirm the stationary point or transition state nature for each optimized geometry. The frequencies were also used later to correct for the zero point vibrational energy (ZPVE). The MP2/6–31G* results were used as input for the final calculation and the geometries reported here were obtained using split valence plus polarization basis set functions (6–31G*) and quadratic configuration interaction with single and double exciations (QCISD). The quadratic CI model is size consistent. The nine valence orbitals and 41 virtual orbitals were used in the CI calculation. Symmetry constraints were avoided for all optimizations and tightened optimization criteria were requested for all SCF calculations. CASSCF(*n*,*m*)/6–31G* optimizations, where *n* is the number of electrons and *m* is the number of orbitals in the complete active space, were performed on all transition states and several of the stable molecules as a comparison to the QCISD/6–31G* optimization.

RESULTS

The complete mapping of the reaction space requires information on a number of stable molecules, e.g. oxirane in ring-closed and ring-opened forms, acetaldehyde, methane, ethylene and carbon monoxide, radicals such as oxygen, methyl and formyl and transition states. In addition, many chemical species may be involved as either singlet or triplet spin states. Table 1 presents the absolute *ab initio* MP2 and QCISD energies of the relevant states of these molecules and also QCISD energies relative to that of ground-state oxirane. Four different transition structures are included to account for the reaction pathways leading from oxirane (S_0) to ground-state singlet acetaldehyde (TSD), acetaldehyde (T_1) to CH_3+HCO (TSC), acetaldehyde (S_0) to CH_4+CO (TSB) and oxirane (S_0) to the ring-opened, CH_2OCH_2 ground-state isomer (TSA). Additional transition states are possible, but those noted suffice for the purposes of this investigation. The optimized QCISD/6–31G* geometries for the stationary state structures are shown in Figure 1 and those for the transition structures are presented in Figure 2. The optimized values of the geometrical parameters are contained in Tables 2 and 3. Zero-point vibrational energy corrections have been included in Table 1 for all structures. When the final products of a reaction channel are separated fragments, the energy of the products was calculated using the isolated fragment geometries (also optimized at the same level of theory) in a 'supermolecule.' In no instance did the geometry of the fragments change, even though all geometric parameters were set as optimizable parameters in the 'supermolecule.'

The inclusion of additional electron configurations in the wavefunction by applying QCISD calculations has a minor impact on the geometries of the molecules in comparison with the MP2 method. In general, only increases in structural parameters were observed and these changes were limited to less than 0·5% of the MP2 values. The only exception to this generalization involved the 2% decrease in all bond angles in the oxirane triplet and the 3% increase in the C—O—C bond angle in TSA. Energetic considerations were more significant. As Table 1 indicates, the energies of all triplet structures, relative to singlet oxirane, decreased by approximately 10% upon application of the CI model, while some, but not all, singlet structures exhibited increase of similar magnitude.

Generally, CI methods or MC-SCF methods are employed for calculations involving radicals. The CI methods are post-SCF and, therefore, are single reference

Table 1. *Ab initio* energies[a] for the relevant stationary and transition states

No.	Molecule	MP2/6–31G*	QCSID/6-31G*	ZPVE[b]	$E_{relative}$ (kcal mol^{-1})
I	*c*-C_2H_4O (S_0)	−153·30358	−153·32850	−153·26964	—
II	*c*-C_2H_4O (T_1)	−153·19123	−153·23805	−153·18305	54·3
III	CH_2OCH_2 (S_0)	−153·22289	−153·24129	−153·18683	52·0
IV	CH_2CH_2O (T_0)	−153·19660	−153·23905	−153·18597	52·5
V	CH_3CHO (S_0)	−153·34691	−153·37337	−153·31641	−29·3
VI	CH_3CHO (T_1)	−153·21044	−153·25350	−153·19848	44·7
	CH_4+CO	−153·35455	−153·38230	−153·32825	−36·8
	$CH_3^{\bullet}+CHO^{\bullet}$	−153·20382	−153·23482	−153·19084	49·4
	C_2H_4+O (^3P)	−153·16506	−153·20925	−153·15721	70·6
VII	TSA	−153·19860	−153·22090	−153·16740	64·2
VIII	TSB	−153·19580	−153·22007	−153·16980	62·7
IX	TSC	−153·18058	−153·22082	−153·16948	62·9
X	TSD	−153·22564	−153·24730	−153·19576	46·4

[a] Energies are in hartrees, except $E_{relative}$, which is expressed in kcal mol^{-1} relative to the energy of oxirane (S_0).
[b] Scaled MP2/6–31G* frequencies used for ZPVE correction to QCISD/6–31G* absolute energies.

methods. MC-SCF techniques simultaneously optimize the coefficients in the wavefunction and the various electron configurations. In order to demonstrate that the QCISD calculations are not in error owing to the lack of additional configurations in the reference state, CASSCF calculations were completed for all transition states as well as a number of the stable configurations. For most calculations, a small number (10) of configurations were involved, but in all cases, one configuration, that used in the single reference SCF, was dominant with a coefficient of the order of $>0{\cdot}97$. The next most important coefficient, *ca* $0{\cdot}12$, mixed in an electronic configuration in which the HOMO electrons (n_O) were both promoted to the LUMO (σ^*). Since TSD is critical to the conclusions of this paper, the complete active space for this geometry was extended and 1764 configurations were included in the SCF calculation. The results for both geometry and energy are presented in Table 4. As is evident, the geometry does vary with the extent of the active space, but no gross changes are encountered. In fact, the only geometry variation is consistent with that typically reported for the QCISD method in comparison with HF. Moreover, as the number of configurations increases, the geometry and the absolute energy tends toward the reported QCISD value. The data in Table 4 validate the selection of the post-SCF CI method in which a very substantial number of configurations are employed with a single reference configuration.

Although not reported here, the normal modes were calculated at the MP2/6–31G* level of theory for all optimized structures. The calculated frequencies for the stable geometries are in good agreement with those published previously using lower levels of theory.[11]

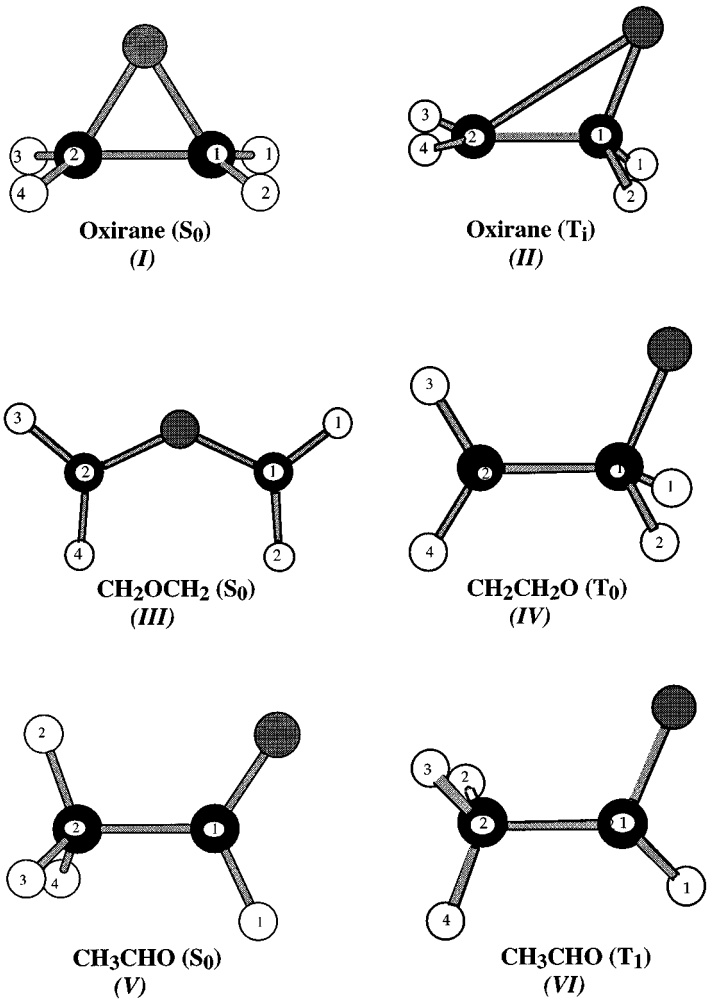

Figure 1. Molecular structures of the 'stable' configurations at the QCISD/6–31G* level of theory

Energies

Comparison may be made between the calculated energies and those previously obtained by theory or experiment. The triplet acetaldehyde is calculated to lie 74·0 kcal mol^{-1} above the ground state in good agreement with the experimentally[18] obtained value of 77·8 kcal mol^{-1}. The $CO+CH_4$ dissociation limit is estimated [calculated from the thermochemistry of the reaction CH_3CHO $(S_0)\rightarrow CH_4+CO$ in the gaseous state; enthalpies of activation obtained from Ref. 19] to be 4·6 kcal mol^{-1} below the ground state of acetaldehyde, but the calculations predict a limit of 7·5 kcal mol^{-1}. The production of CH_3+HCO lies 83·0 kcal mol^{-1} above CH_3CHO (S_0), 4·3 kcal mol^{-1} higher than the *ab initio* calculations predict [calculated from the thermochemistry of the reaction CH_3CHO $(S_0)\rightarrow CH_3^{\bullet}+HCO^{\bullet}$ in the gaseous state; enthalpies of activation obtained from Ref. 19]. The barrier to the dissociation of $CH_3CHO(T_1)$ has been estimated experimentally[20] as 14 kcal mol^{-1}, in good agreement, given the

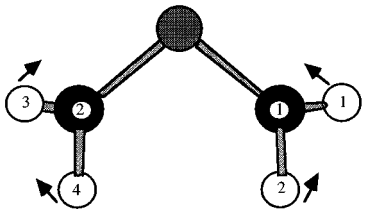

TSA
(VII)

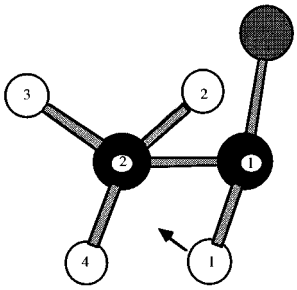

TSB
(VII)

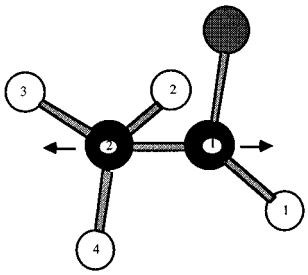

TSC
(IX)

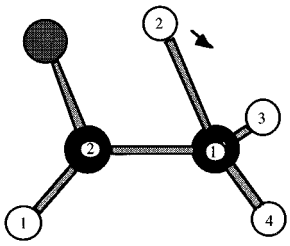

TSD
(X)

Figure 2. Molecular structures of the transition state configurations at the QCISD/6–31G* level of theory

Table 2. Geometric parameters for oxirane-like structures

Parameter	S_0	T_1	CH_2OCH_2	CH_2CH_2O	TSA	TSD
C_2—O	1·435	2·431	1·315	1·491[a]	1·363	1·414[a]
C_1—O	1·435	1·407	1·315	1·393	1·363	1·291
C_1—H_1	1·091	1·100	1·085	1·104	1·083	1·094
C_1—H_2	1·091	1·100	1·079	1·116	1·085	1·528
C_2—H_3	1·091	1·087	1·085	1·086	1·086	1·090
C_2—H_4	1·091	1·087	1·079	1·086	1·083	1·094
∠C—O—C	61·52	34·10	128·76	112·64[b]	104·37	110·35[b]
∠C—C—H_1	115·24	111·14	119·82	111·43	118·28	130·97
∠C—C—H_2	115·24	111·11	115·00	102·82	117·10	66·55
∠C—C—H_3	115·24	106·25	119·82	92·90	117·07	121·20
∠C—C—H_4	115·24	106·21	115·01	143·65	118·24	112·14
∠C_2—O—C_1—H_1	110·91	113·48	−1·52	−127·17	43·68	−182·34[c]
∠C_2—O—C_1—H_2	−110·91	−113·48	−177·25	120·38	−232·27	−9·45[c]
∠C_1—O—C_2—H_3	−110·91	−123·99	−177·40	−146·64	127·42	206·28[c]
∠C_1—O—C_2—H_4	110·91	123·97	−1·47	59·31	−43·28	67·74[c]

[a] C_1—C_2, [b] ∠C_1—C_2—O and [c] ∠C—C—O—H, since these quantities are more meaningful for the structures.

experimental uncertainties, with the predicted value of 18·2 kcal mol^{-1} reported here. Oxirane is estimated,[21] by thermochemical calculations, to lie 27·3 kcal mol^{-1} above the ground state of acetaldehyde. The computations predict a value of 29·3, in excellent agreement with this estimate. The ring-opened forms of oxirane are predicted to be considerably less stable than the ring-closed form. The ether-like CH_2OCH_2 isomer in its ground state (S_0) is calculated to lie 52·0 kcal mol^{-1} above the ring-closed form. The vinyl alcohol-like CH_2CH_2O ground state (T_0) lies 52·5 kcal mol^{-1} higher than the ring-closed isomer according to the calculations. We note that attempts to optimize the geometry of the lowest singlet state of CH_2CH_2O collapsed to the ground-state acetaldehyde structure. There are no experimental data with which to compare these estimates; however, the accuracy of the calculations for which experimental data exist bodes well for the computational predictions. In general, the *ab initio* calculations overestimate the locations of the molecular dissociation limits and underestimate the locations of the radical dissociation limits.

Table 3. Geometric parameters for acetaldehyde-like structures

Parameter	S_0	T_1	TSB	TSC
C_1—C_2	1·508	1·514	2·077	2·047
C_2—O	1·219	1·340	1·186	1·222
C_1—H_1	1·111	1·099	1·095	1·121
C_2—H_2	1·098	1·100	1·093	1·088
C_2—H_3	1·094	1·095	1·093	1·086
C_2—H_4	1·098	1·096	1·097	1·088
∠C_1—C_2—O	124·27	114·45	106·82	105·59
∠C_2—C_1—H_1	115·43	117·80	56·18	90·65
∠C_2—C_1—H_2	109·88	111·88	98·49	103·55
∠C_2—C_1—H_3	109·84	109·06	98·41	99·67
∠C_2—C_1—H_4	109·88	110·27	123·36	100·93
∠C_2—C_1—O—H_1	180·00	−133·31	180·10	124·09
∠C_2—C_1—O—H_2	121·11	64·00	56·77[a]	300·10[a]
∠C_1—C_2—O—H_3	0·00	184·45	−57·18	59·92
∠C_1—C_2—O—H_4	−121·10	−56·45	−0·06	−56·81

[a] C_1—C_2—O—H_2 is the appropriate angle for this structure.

Geometries

The geometric parameters for each molecule are contained in Tables 2 and 3. For ground-state oxirane the agreement is excellent.[22] The correlated method results are within 0·005 Å for bond lengths and 0·1° for bond angles of the reported experimental values. Agreement between the *ab initio* results and the experimental values for the ground-state acetaldehyde molecule falls within the same limits. Although the experimental geometries for the transition states of these molecules are unknown, the excellent agreement for the ground states also lends confidence to the values for these states. Similar claims may be made for the geometries of the ring-opened forms of oxirane also contained in Table 2.

Transition states

The geometries of the transition states are presented numerically in Tables 2 and 3 and graphically in Figure 2. The reaction coordinates are indicated by arrows in the figure.

TSA, the transition state connecting the ring-closed and ether-like ring-opened forms, is a structure intermediate in geometry between the two stationary states it joins. The C—O—C bond angle has increased significantly (*ca* 70% greater than S_0); however, the hydrogen atoms are in essentially their ring-closed position and motion over the reaction barrier involves counter-rotation of these two sets

Table 4. Compared of computational methods for transition state D

Parameter	SCF	CAS(2,2)	CAS(4,4)	CAS(6,6)	CAS(8,8)	QCISD
C_1—C_2	1·421	1·427	1·418	1·417	1·418	1·414
C_2—O	1·252	1·257	1·261	1·288	1·290	1·291
C_1—H_1	1·081	1·080	1·080	1·080	1·079	1·094
C_1—H_2	1·519	1·567	1·550	1·552	1·583	1·528
C_2—H_3	1·079	1·079	1·079	1·079	1·079	1·090
C_2—H_4	1·085	1·085	1·084	1·083	1·083	1·094
∠C—C—O	109·18	109·05	110·32	110·01	111·18	110·35
∠C—C—H_1	131·55	132·62	131·34	131·87	130·69	130·97
∠C—C—H_2	65·61	64·60	65·47	65·39	66·01	66·55
∠C—C—H_3	120·71	119·68	120·21	120·12	120·13	121·20
∠C—C—H_4	110·03	110·29	111·07	111·34	111·54	112·14
∠C_2—C_1—O—H_1	−182·73	−181·88	−182·71	182·88	−181·90	−182·34
∠C_2—C_1—O—H_2	−7·94	−6·61	−8·12	−8·42	−8·15	−9·45
∠C_1—C_2—O—H_3	−207·57	209·39	207·40	207·51	205·76	206·28
∠C_1—C_2—O—H_4	73·71	77·11	72·66	72·32	70·32	67·74
Energy (a.u.)	−152·77082	−152·79308	−152·82919	−152·87649	−152·89674	−153·24730
Ref. configurations	n/a	3	20	175	1764	n/a

of atoms. TSB connects ground-state acetaldehyde with the CH_4+CO products. The transition-state geometry is reactant-like in structure and the reaction coordinate involves a vibration-like motion to transfer a hydrogen atom to the carbon that will be in the methane molecule. TSC, which connects triplet acetaldehyde to the radical products CH_3+HCO, is also reactant-like in its geometry and the reaction coordinate is a bond stretching vibration, as would be expected. TSD is a transition state which joins the ground-state oxirane and acetaldehyde isomers. In contrast to the transition states along the acetaldehyde potential surface, this structure is product-like in its geometry. The hydrogen atom to be transferred has an increased bond length and may be envisioned as partially bound to both of the carbon atoms. The reaction coordinate is a vibration leading to bond shortening of a C—H bond on the carbon atom to which the hydrogen is transferring.

DISCUSSION

With the help of Figure 3, we may explore the nature of the possible reaction pathways beginning with oxirane in the ground singlet electronic state. The lowest oxirane triplet state lies *ca* 55 kcal mol^{-1} above S_0. The transition state (TSD) connecting oxirane (S_0) and CH_3CHO (S_0) is *ca* 8 kcal mol^{-1} lower in energy. Given the high temperatures and long irradiation times in the reported experiments discussed in the Introduction, there is a high probability of resonant V–V energy transfer and either TSD or the triplet oxirane is attainable from S_0. Assuming that all of the energy needed to traverse the transition state is available, the lowest energy passage along the ground state potential surface would produce singlet acetaldehyde in a highly excited vibrational state. The vibrationally hot CH_3CHO may energetically undergo intersystem crossing to the triplet state. Alternatively, the transition state for fragmentation of the ground state acetaldehyde to CH_4 and CO, TSB, is located *ca* 16 kcal mol^{-1} above TSD. There would not be a significant energetic barrier to the formation of these molecular products. Indeed, the dominant products in one of the experimental studies[5] were methane and carbon monoxide. Turning to the CH_3CHO (T_1) intersystem crossing product, one notes from Figure 3 that the transition state for production of radical products, TSC, is nearly isoenergetic with the transition state leading to molecular products. Given the nature of the radiative and collisional energy transfer, these two reactions are, energetically, equally probable. Production of the acetaldehyde triplet molecule directly from triplet oxirane appears to be an unlikely process. The transition state for this reaction could not be located with the QCISD/6–31G* theoretical model, but using MP2/6–31G* calculations, lies nearly 40 kcal mol^{-1} above TSD or more than 100 kcal mol^{-1} above the ground-state oxirane, so that even if the reaction conditions led to triplet oxirane formation, the energetics would result in a vanishingly small reaction rate from that state to acetaldehyde.

The formation of the ring-opened isomers of oxirane and molecular products such as formaldehyde also appears to be an unfavorable process. TSA lies *ca* 18 kcal mol^{-1} above TSD; however, the endoergicity for formation of the ether-like form of oxirane is very large. The activation barrier for reformation of the ring-closed isomer is predicted to be only 12 kcal mol^{-1} and, energetically, this process would easily occur. We could not locate a transition state between the triplet state of the ring-closed form of oxirane and the vinyl alcohol-like isomer. This is in agreement with a lower level study of oxirane.[7,8] Therefore, formation of any quantity of CH_2CH_2O (in its lowest electronic state, a triplet) would be followed by immediate ring-closure back to oxirane, since there would be no activation barrier to the reverse process. Nor could we locate a transition state on the surface

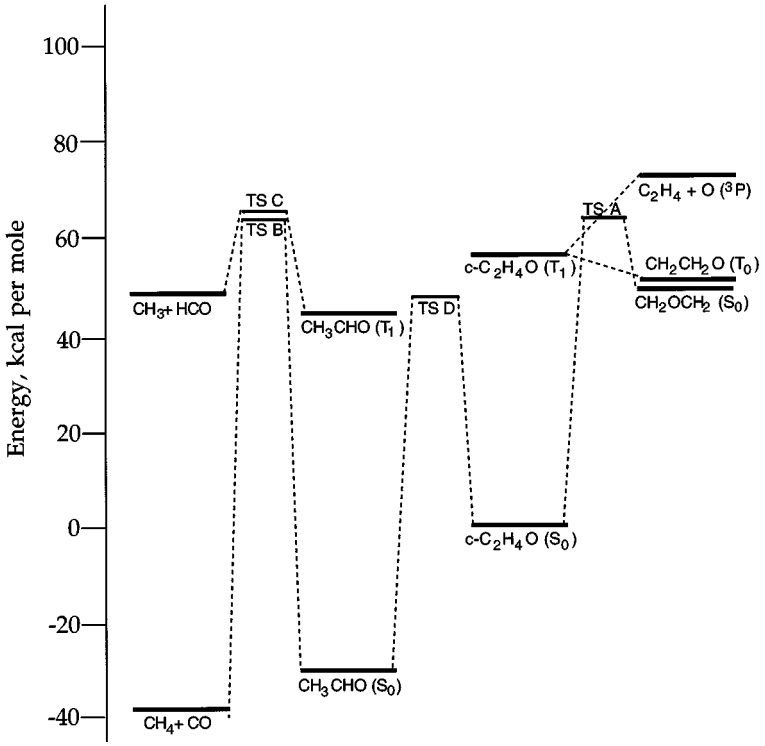

Figure 3. Schematic representation of the reaction pathways for the oxirane system. Energies were obtained by an QCISD/6–31G* model with ZPVE corrections

connecting the ring-closed triplet isomer with $C_2H_4 + O(^3P)$. The fate of any such product would be identical with that just described for CH_2CH_2O.

Based on the analysis of the energetics of the isomers of C_2H_4O and the relevant transition states, one would conclude that the CH_4 and CO products are a result of a primary reaction process that produces ground-state acetaldehyde. Secondary reactivity of this vibrationally hot acetaldehyde results in the formation of the molecular products. Radical products are produced from the secondary chemistry of triplet acetaldehyde produced by intersystem crossing from the primary product. Recombination of the methyl radicals, followed by additional secondary processes, leads to formation of the unsaturated products observed experimentally and unimolecular reaction of the formyl radical leads to formation of H_2 and CO.

CONCLUSION

The information presented in this paper does not necessarily lead to a unique mechanism for the observed reactivity. However, a possible, kinetic pathway is outlined in Figure 3. All of the final products may be derived from the same primary product. This product, shown to be acetaldehyde (S_0), undergoes further unimolecular decomposition to produce one set of molecular products (CH_4 and CO) products or undergoes intersystem crossing to the triplet. The second set of products results indirectly from the unimolecular reactivity of the lowest triplet state of acetaldehyde. The latter produces $CH_3 + HCO$, with subsequent formation of CO and C_2H_6. This model predicts that the relative yield of CO should equal that of the sum of all other products, as was typically observed in the experimental results.

ACKNOWLEDGEMENTS

The Chemistry Department IBM RISC-6000 computer facilities were established with support from the Camille and Henry Dreyfus Foundation, the Keck Foundation and IBM. Support was also provided by the Pittsburgh Supercomputing Center (Grant CHE950013P), which is funded by the National Science Foundation.

REFERENCES

1. K. H. Mueller and W. D. Walters, *J. Am. Chem. Soc.* **73**, 1458 (1951).
2. I. Crocco, I. Glassman and I. E. Smith, *J. Chem. Phys.* **31**, 506 (1959).
3. M. L. Neufeld and A. T. Blades, *Can. J. Chem.* **41**, 2956 (1963).

4. S. W. Benson, *J. Chem. Phys.* **40**, 105 (1964).
5. A. Lifshitz and H. Ben-Hamou, *J. Phys. Chem.* **87**, 1782 (1983).
6. O. P. Strausz and R. K. Gosavi, *Prog. Theor. Org. Chem.* **2**, 248 (1977).
7. B. Bigot, A. Sevin and A. Devaquet, *J. Am. Chem. Soc.* **101**, 1095 (1979).
8. B. Bigot, A. Sevin and A. Devaquet, *J. Am. Chem. Soc.* **101**, 1101 (1979).
9. W. J. Bouma, L. Radom and W. R. Rodwell, *Theor. Chim. Acta* **56**, 149 (1980).
10. K. Yamaguchi, S. Yabushita, T. Fueno, S. Kato and K. Morokuma, *Chem. Phys. Lett.* **70**, 27 (1980).
11. J. A. Altmann, T. A. M. Doust and A. D. Osborne, *Chem. Phys. Lett.* **69**, 595 (1980).
12. M. R. Peterson, G. R. DeMare, I. G. Csizmadia and O. P. Strausz, *J. Mol. Struct.* **92**, 239 (1983).
13. J. S. Yadav and J. D. Goddard, *J. Chem. Phys.* **84**, 2682 (1986).
14. E. D. Simandiras, R. D. Amos, N. C. Handy, T. J. Lee, J. E. Rice, R. B. Remington and H. F. Schaefer, *J. Am. Chem. Soc.* **110**, 1388 (1988).
15. C. M. Hadad, J. B. Foresman and K. B. Wiberg, *J. Phys. Chem.* **97**, 4293 (1993).
16. J. Simons, *J. Phys. Chem.* **95**, 1017 (1991).
17. M. J. Frisch, G. W. Trucks, M. Head-Gordon, P. M. W. Gill, M. W. Wong, J. B. Foresman, B. G. Joohnson, H. B. Schlegel, M. A. Robb, E. S. Replogle, R. Gomperts, J. L. Andres, K. Raghavachari, J. S. Binkley, C. Gonzalez, R. L. Martin, D. J. Fox, D. J. Defrees, J. Baker, J. J. P. Stewart and J. A. Pople, *Gaussian 92, Revision C.* Gaussian, Pittsburgh, PA (1992).
18. D. C. Moule and K. H. K. Ng, *Can. J. Chem.* **63**, 1378 (1985).
19. F. T. Wall, *Chemical Thermodynamics*, 3rd edn. Freeman, San Francisco (1974).
20. A. Horowitz, C. J. Kershner and J. G. Calvert, *J. Phys. Chem.* **86**, 3094 (1982); A. Horowitz and C. G. Calvert, *J. Phys. Chem.* **86**, 3105 (1982).
21. G. L. Cunningham, A. W. Boyd, R. J. Myers, W. D. Gwinn and W. I. LeVan, *J. Chem. Phys.* **19**, 676 (1951); C. Hirose, *Bull. Chem. Soc. Jpn.* **47**, 1311 (1974).
22. M. D. Harmony, V. W. Laurie, R. I. Kuczkowski, R. H. Schwendemann, D. A. Ramsey, W. J. Lovas, W. J. Lafferty and A. G. Maki, *J. Phys. Chem. Ref. Data* **8**, 619 (1979).

